JOC *Article*

# Structure, Conformation, and Stereodynamics of the Atropisomers of Highly Hindered Benzyl Ethers

Daniele Casarini,[†] Carmine Coluccini,[1,‡] Lodovico Lunazzi,[‡] and Andrea Mazzanti*,[‡]

*Department of Chemistry, University of Basilicata, Potenza, Italy, and Department of Organic Chemistry "A. Mangini", University of Bologna, Viale Risorgimento, 4 Bologna 40136, Italy*

*mazzand@ms.fci.unibo.it*

*Received February 15, 2006*

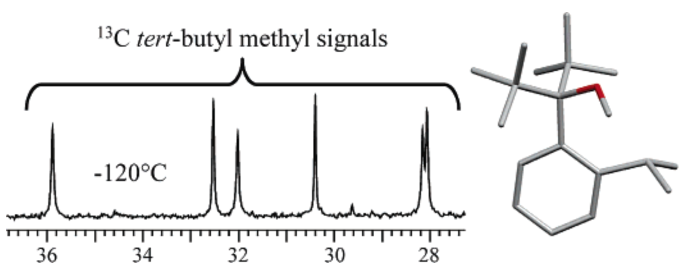


Low-temperature and NOE NMR spectra of four of the title compounds indicate that they adopt a synclinal (sc) conformation, in agreement with the prediction of ab initio computations. In the case of the most-hindered derivative (compound **4**), the conformation is syn-periplanar (sp), as is also shown by X-ray diffraction. Such stereolabile sp- or sc-atropisomers exist as two conformational enantiomers: the corresponding enantiomerization barriers, covering the range 6.6 to 9.7 kcal mol$^{-1}$, could be measured for all the examined compounds. In two cases (compounds **3** and **5**), the minor antiperiplanar (ap) atropisomer has been also observed, and the sc to ap interconversion barrier measured (11.7 and 11.9 kcal mol$^{-1}$, respectively). In addition, restricted rotation of the isopropyl and *tert*-butyl substituents has been detected, and the corresponding barriers have been determined.

## Introduction

It has been reported that carbinols of the type Ar−C(OH)$R_2$ exhibit significant restricted rotation about the $sp^2$−$sp^3$ bond,[2−10] which originates stereolabile atropisomers when the aryl moiety does not possess a local 2-fold symmetry axis.[3,5−8,10] If the OH moiety is replaced by the bulkier −OMe group, the increased dimension is expected to affect significantly the conformational behavior, so that dynamic features, not observable in the corresponding carbinols, should be detectable. We thus investigated here the methylbenzyl ethers **1**−**5**, bearing substituents of different bulkiness (Chart 1). In all the examined compounds an isopropyl group has been introduced to have a NMR probe suitable to detect the molecular asymmetry at the $^{13}$C frequency.

**CHART 1**

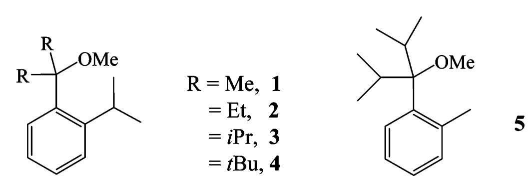


[†] University of Basilicata.
[‡] University of Bologna.
(1) In partial fulfillment for the PhD in Chemical Sciences, University of Bologna.
(2) (a) Newsoroff, G. P.; Sternhell, S. *Tetrahedron Lett*. **1967**, 2539. (b) Baas, J. M. A.; Sinnema, A. *Recl. Trav. Chim. Pays-Bas* **1973**, *92*, 899. (c) Baas, J. M. A.; van der Toorn, J. M.; Wepster, B. M. *Recl. Trav. Chim. Pays-Bas* **1974**, *93*, 173.
(3) (a) Landman, D.; Newsoroff, G. P.; Sternhell, S. *Aust. J. Chem.* **1972**, *25*, 109. (b) Suezawa, H.; Wada, H.; Watanabe, H.; Yuzuri, T.; Sakakibara, K.; Hirota, M. *J. Phys. Org. Chem.* **1997**, *10*, 925.
(4) Anderson, S.; Drakenberg, T. *Org. Magn. Reson.* **1983**, *21*, 730.
(5) Lomas, J. S.; Dubois, J.-E. *J. Org. Chem.* **1976**, *41*, 3033. Lomas, J. S.; Luong, P. K.; Dubois, J.-E. *J. Org. Chem.* **1977**, *42*, 3394.
(6) Lomas, J. S.; Dubois, J.-E. *Tetrahedron* **1981**, *37*, 2273. Lomas, J. S.; Vaissermsnn, J. *J. Chem. Soc., Perkin Trans. 2* **1998**, 1777. Lomas, J. S. *J. Chem. Soc., Perkin Trans. 2* **2001**, 754. Lomas, J. S.; Adenier, A. *J. Chem. Soc., Perkin Trans. 2* **2002**, 1264.
(7) (a) Anderson, J. E.; Bru-Capdeville, V.; Kirsch, P. A.; Lomas, J. S. *Chem. Commun.* **1994**, 1077. (b) Lomas, J. S.; Anderson, J. E. *J. Org. Chem.* **1995**, *60*, 3246.
(8) Casarini, D.; Lunazzi, L.; Mazzanti, A. *J. Org. Chem.* **1997**, *62*, 3315.
(9) Wolf, C.; Pranatharthiaran, L.; Ramagosa, R. B. *Tetrahedron* **2002**, *43*, 8567.
(10) Casarini, D.; Coluccini, C.; Lunazzi, L.; Mazzanti, A. *J. Org. Chem.* **2005**, *70*, 5098.

10.1021/jo0603173 CCC: $33.50 
Published on Web 05/18/2006

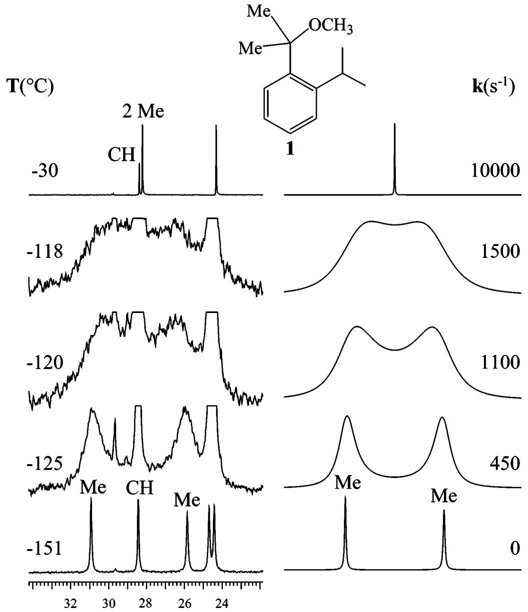


**FIGURE 1.** Left: 24 to 32 ppm region of the $^{13}$C NMR spectrum of **1** (150.8 MHz in $CHF_2Cl/CHFCl_2$) showing the splitting of the methyl signals at −151 °C. The two unlabeled signals at 24.4 and 24.6 ppm are those of the isopropyl methyl groups that are diastereotopic at −151 °C as a result of the conformation being chiral at this temperature. Right: simulation of the two lines of the methyl groups bonded to the C−OMe moiety.

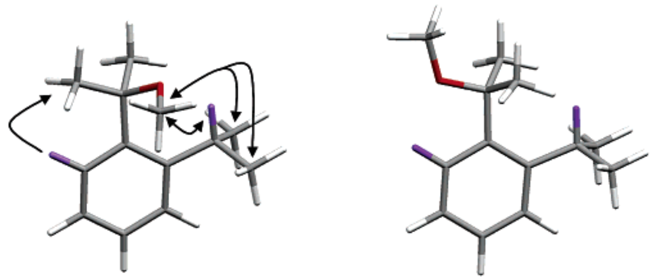

**1** (sc-atropisomer) E = 0.0    **1** (ap-atropisomer) E = 3.4

**FIGURE 2.** Ab initio computed structures of the sc- (left) and ap-atropisomer (right) of **1** (the relative computed energies are in kcal mol$^{-1}$). The observed NOE effects are also indicated in the case of the sc-atropisomer (see text).

**TABLE 1. Experimental Barriers (Δ$G^‡$ in kcal mol$^{-1}$) Measured in Compounds 1−5**

| compd | sc to ap interconversion | enantiomerization | isopropyl rotation | *tert*-butyl rotation |
|---|---|---|---|---|
| **1** | | 6.6 | | |
| **2** | | 9.7 | | |
| **3** | 11.9 | 9.1 | ≥11.9 (ap-atropisomer)<br>6.9 (sc-atropisomer) | |
| **4** | | 8.4 | | 9.4 |
| **5** | 11.7 | 8.8 | 7.8 (ap-atropisomer) | |

## Results and Discussion

When the $^{13}$C spectrum of **1** is recorded at temperatures lower than −100 °C, the isopropyl methyl signals, and that of the methyl bonded to the C−OMe moiety, broaden considerably and eventually split into pairs of equally intense lines at −151 °C (Figure 1), whereas all the other carbons display single lines at any temperature. This indicates that the rotation about the Ar−C bond has been frozen in the NMR time scale and that the molecule has adopted an asymmetric, thus chiral, conformation (it is for this reason that the isopropyl methyl groups become diastereotopic at this temperature).

According to ab initio calculations (Experimental Section), two energy minima, corresponding to two possible conformers (stereolabile atropisomers), are available to compound **1**. The more stable ($E = 0$) conformer is that having a synclinal (sc) conformation,[11] where the dihedral angle $\vartheta$ between the planes identified by C1−C−OMe and by the benzene ring (i.e., the C2−C1−C−OMe dihedral angle) is equal to 42° (Figure 2), whereas the less stable ($E = 3.4$ kcal mol$^{-1}$) is that exhibiting an antiperiplanar (ap) situation, where the mentioned dihedral angle $\vartheta$ is about 180°. Whereas the sc-atropisomer does not have any element of symmetry, the ap-atropisomer displays a plane of symmetry and, for this reason, cannot account for the NMR spectrum observed at −151 °C. The absence of signals corresponding to a second form implies that the population of the symmetric ap-atropisomer is negligible (in agreement with the computed high-energy value), so that the sc-atropisomer is essentially the only populated form of compound **1**.[12]

An additional proof that the asymmetric atropisomer has the sc type of structure is offered by NOE experiments, that were carried out at −20 °C to maximize the effects of the enhancement. As indicated in Figure 2 (left), irradiation of the CH and Me signals of the isopropyl group enhances the OMe singlet and vice versa. Also, irradiation of the H-6 multiplet of the aromatic ring gives an almost negligible effect on the OMe singlet but a quite large effect on the signal of the methyl groups bonded to the C−OMe moiety.

Line shape simulation yields the rate constants, hence, the free energy of activation (Δ$G^‡$ = 6.6 kcal mol$^{-1}$, as in Table 1) for the dynamic process responsible for the exchange of the methyl signals.[13] This process corresponds to the interconversion of the atropisomer +sc into its enantiomeric form −sc. There are two possible routes for achieving such interconversion: either the OMe group crosses over the isopropyl group or crosses over the hydrogen in position 6 of the benzene ring.[14] According

(11) Eliel, L. E.; Wilen, S. H. *Stereochemistry of Organic Compounds*; John Wiley and Sons: New York, 1994; p 21.

(12) This result is at variance with the finding observed in the analogous carbinol derivative,[10] where the minor ap-atropisomer was sufficiently populated (about 23%) to be experimentally observed.

(13) As is often observed in the conformational process, the Δ$G^‡$ value was found independent of temperature within the experimental uncertainty of the NMR measurements. See: Hoogosian, S.; Bushweller, C. H.; Anderson, W. G.; Kigsley, G. *J. Phys. Chem.* **1976**, *80*, 643. Lunazzi, L.; Cerioni, G.; Ingold, K. U. *J. Am. Chem. Soc.* **1976**, *98*, 7484. Forlani, L.; Lunazzi L.; Medici, A. *Tetrahedron Lett.* **1977**, *18*, 4525. Bernardi, F.; Lunazzi, L.; Zanirato, P.; Cerioni, G. *Tetrahedron* **1977**, *33*, 1337. Lunazzi, L.; Magagnoli, C.; Guerra, M.; Macciantelli, D. *Tetrahedron Lett.* **1979**, 3031. Cremonini, M. A.; Lunazzi, L.; Placucci, G.; Okazaki, R.; Yamamoto, G. *J. Am. Chem. Soc.* **1990**, *112*, 2915. Anderson, J. E.; Tocher, D. A.; Casarini, D.; Lunazzi, L. *J. Org. Chem.* **1991**, *56*, 1731. Borghi, R.; Lunazzi, L.; Placucci, G.; Cerioni, G.; Foresti, E.; Plumitallo, A. *J. Org. Chem.* **1997**, *62*, 4924. Garcia, M. B.; Grilli, S.; Lunazzi, L.; Mazzanti, A.; Orelli, L. R. *J. Org. Chem.* **2001**, *66*, 6679. Garcia, M. B.; Grilli, S.; Lunazzi, L.; Mazzanti, A.; Orelli, L. R. *Eur. J. Org. Chem.* **2002**, 4018. Casarini, D.; Rosini, C.; Grilli, S.; Lunazzi, L.; Mazzanti, A. *J. Org. Chem.* **2003**, *68*, 1815. Casarini, D.; Grilli, S.; Lunazzi, L.; Mazzanti, A. *J. Org. Chem.* **2004**, *69*, 345. Bartoli, G.; Lunazzi, L.; Massacesi, M.; Mazzanti, A. *J. Org. Chem.* **2004**, *69*, 821. Casarini, D.; Coluccini, C.; Lunazzi, L.; Mazzanti, A.; Rompietti, R. *J. Org. Chem.* **2004**, *69*, 5746.

(14) In the course of the latter pathway, the mentioned ap-atropisomer would be visited, but as predicted by calculations, its population is too low to be experimentally detectable.

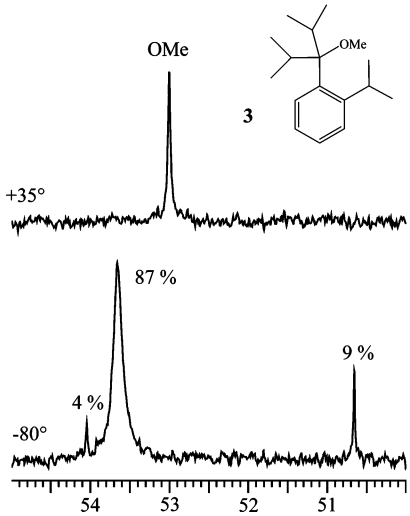


**FIGURE 3.** $^{13}C$ NMR signals (150.8 MHz) of the OMe group of **3** in toluene-$d_8$ at two different temperatures.

to ab initio calculations, the energies of the transition states due to these two processes are, respectively, 5.3 and 9.8 kcal $mol^{-1}$ higher than the energy of the ground state. As a consequence, the enantiomerization is expected to follow a pathway where the OMe crosses over the isopropyl group, because this process has a lower transition energy and, also, has a theoretical barrier closer to the experimental value (5.3 vs 6.6 kcal $mol^{-1}$).

It is worth outlining that in the analogous carbinol derivative[10] such an enantiomerization process was too fast in the NMR time scale to be experimentally detected, even at −150 °C: in the case of **1**, the presence of the OMe group, bulkier than OH, makes the enantiomerization barrier sufficiently high to be determined by NMR.

An analogous behavior is observed for compound **2** (R = Et), where the isopropyl methyl carbons and the carbons of the ethyl groups (both $CH_2$ and $CH_3$) become diastereotopic at −120 °C. Again, only the asymmetric atropisomer, to which the sc type of structure was assigned, is observed at low temperature. Computations in fact indicate that this conformer (where the mentioned C2−C1−C−O dihedral angle $\vartheta$ is 45°) is more stable by 1.4 kcal $mol^{-1}$ than the symmetric ap-atropisomer, where the $\vartheta$ angle is 180°. As in the previous case, the NOE experiment confirms the sc type of structure, because irradiation of the Me and CH signals of the isopropyl substituent enhances the OMe singlet as well as the $CH_2$ signal of the ethyl group, and irradiation of the H-6 signal of the aromatic ring shows NOE effect on the $CH_2$ multiplet but not on the OMe singlet.

Line-shape simulation indicates that the enantiomerization process for interconverting the +sc into the −sc enantiomer has a barrier of 9.7 kcal $mol^{-1}$ (Table 1): this value is larger than that measured for **1** as a result of the greater dimension of the ethyl with respect to the methyl groups bonded to the C−O moiety.

A quite different conformational behavior is observed in the case of **3** (R = *i*-Pr) as a result of the rather severe hindrance generated by the two geminal isopropyl groups bonded to the C−O carbon. The $^{13}C$ single line of the OMe group, in fact, broadens on cooling and splits into three lines at −80 °C: the corresponding shifts being 53.7, 50.7, and 54.0 ppm, with relative intensities of 87:9:4, respectively (Figure 3).

Contrary to the previous cases, therefore, three different conformers appear to be populated in compound **3**. The CH

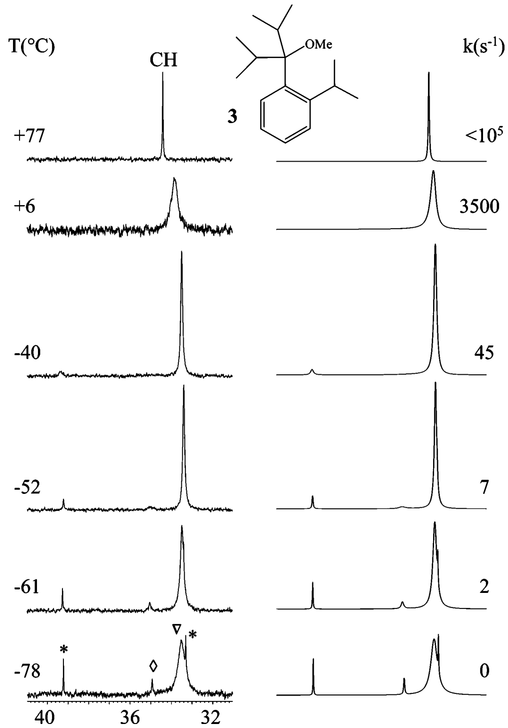


**FIGURE 4.** Left: temperature dependence of the $^{13}C$ NMR signals (150.8 MHz in toluene-$d_8$) of the methine carbon signals of the two geminal isopropyl substituents of **3**. In the trace at −78 °C the triangle indicates the major conformer (87%), the diamond indicates the 4% conformer, and the two stars indicates the two lines of the 9% conformer. Right: line-shape simulations obtained with the rate constants indicated.

signals of the two geminal isopropyl groups yield additional information concerning the symmetry of these conformers. As shown in Figure 4 (trace at −78 °C), the major (87%) and minor (4%) conformers display a single line each for the two geminal isopropyl CH carbons (33.9 and 34.7 ppm, respectively), whereas the conformer with a 9% population displays a pair of CH lines of equal intensity at 39.1 and 33.5 ppm.

Ab initio computations predict the existence of three energy minima corresponding to three atropisomers. That with the lowest energy has a sc-type of structure,[11] with the dihedral angle $\vartheta$ between the C−O−Me plane and the aryl ring (i.e., C2−C1−C−OMe) equal to 38°. Thus, the single line observed for the two geminal isopropyl methine carbons at −78 °C must be a consequence of the rapid interconversion, at this temperature, between the +sc and the −sc enantiomers (Chart 2). This motion creates in fact a dynamic plane of symmetry that renders the CH carbons equivalent (enantiotopic): this symmetry is also a consequence of the fast C−*i*-Pr bond rotation at this temperature. Such an interpretation will be supported by additional experiments described in the following paragraphs.

The other two energy minima predicted by calculations correspond to two different atropisomers, both with an ap-type[11] of structure, where the Me−O−C and the aryl planes are nearly coplanar, with the computed dihedral angle $\vartheta$ being 164° in one atropisomer and 176° in the other.

The ap-atropisomer with the second highest relative energy[15] ($E$ = 2.6 kcal $mol^{-1}$, as in Chart 2) should correspond to the second populated (9%) conformer detected in the NMR experiment of Figure 4. Calculations indicate that in this ap-atropisomer the two geminal isopropyl groups adopt two

**CHART 2**[a]

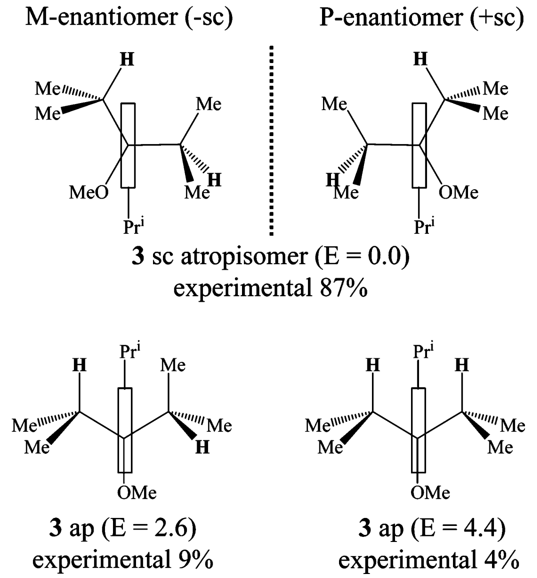


[a] Energies (*E*) are in kcal mol$^{-1}$.

different positions with respect to the −OMe substituent. If the C−*i*-Pr bond rotation is frozen at −80 °C, the two geminal CH carbons will be diastereotopic, in agreement with the two lines experimentally observed. The fact that, contrary to the case of the major sc-atropisomer, the MeOC−*i*-Pr bond rotation is locked in this case at −80 °C, is a consequence of the much higher steric hindrance experienced by the two geminal isopropyl groups in the ap-atropisomer with respect to the sc-atropisomer.

The third computed energy minimum ($E = 4.4$ kcal mol$^{-1}$, as in Chart 2)[15] should correspond to the least populated (4%) atropisomer experimentally observed. The ap-type structure computed for the latter indicates that the two geminal isopropyl groups are symmetrically placed with respect to the −OMe substituents. Thus, even if the MeOC−*i*-Pr bond rotation is frozen at −78 °C, as in the case of its equally hindered ap companion, the two geminal CH carbons will be equivalent (enantiotopic). This agrees with the experimental observation of a single CH line for the minor (4%) conformer.

A line-shape simulation of the three OMe signals (Figure 3) yields the rate constants, hence, the interconversion barrier ($\Delta G^{\ddagger} = 11.9$ kcal mol$^{-1}$, as in Table 1), for the exchange of the atropisomers. The same value is obtained from the simulation of the exchanging lines of the two geminal CH carbons (Figure 4). This barrier, therefore, corresponds to the rotation process about the Ar−COMe bond, which is responsible for the interconversion of the three atropisomers. This barrier must be equal to or lower than that involving the rotation about the MeOC−*i*-Pr bond in the ap-atropisomer (Table 1). In fact, when the distinguishable lines of the geminal isopropyl CH carbons are observed at −78 °C for the three atropisomers, the one with the 9% population already displays diastereotopic CH carbons. Because of this occurrence, the MeOC−*i*-Pr rotation barrier of 3 cannot be measured experimentally, and only its lower limit (i.e., 11.9 kcal mol$^{-1}$, as in Table 1) can be indicated.

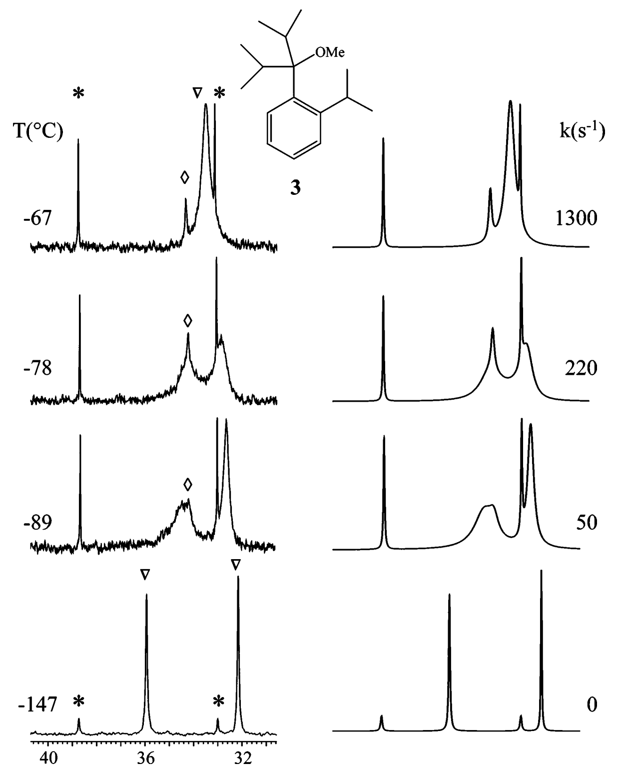


**FIGURE 5.** Left: temperature dependence of the $^{13}$C NMR signals (150.8 MHz in $CHF_2Cl/CHFCl_2$) of the methine carbons of the two geminal isopropyl substituents of **3** (the lines are identified by the same symbols as in Figure 4). Right: line-shape simulations obtained with the rate constants indicated.

When a solvent capable of reaching much lower temperatures is used (i.e., $CHF_2Cl/CHFCl_2$ ), the spectrum of **3** at −67 °C is similar to that observed in toluene at −78 °C, whereas at −78 °C, the major atropisomer (87%) displays two broad lines of equal intensity for the two geminal CH carbons,[16] as shown in Figure 5. The presence of these two lines proves that the +sc to −sc enantiomerization process mentioned above has become slow in the NMR time scale. A line-shape simulation provides a barrier of 9.1 kcal mol$^{-1}$ for this interconversion. This value is larger than the barrier for the analogous process measured in **1** (where it was 6.6 kcal mol$^{-1}$) but somewhat lower than that (9.8 kcal mol$^{-1}$) found in compound **2**. Although the isopropyl is bulkier than the methyl and ethyl groups, the fact that the barrier of **3** is not larger than the analogous barrier of **2** can be explained by considering that the isopropyl group is bulk enough as to destabilize the ground state of the sc-atropisomer of **3** more than its transition state: the energy difference between the ground and the transition state thus becomes lower in **3** with respect to **2**. The occasional lowering of the rotation barrier on increasing the bulkiness of the substituent has been documented.[17]

(15) On a qualitative point of view, the trend of the computed energies (i.e., 0, 2.6, and 4.4 kcal mol$^{-1}$) parallels that of the experimental intensities for the corresponding conformers (i.e., 87, 9, and 4%). However, the computed energy differences are higher than required to quantitatively account for the observed populations. This depends on the computing approximations and on the fact that calculations refer to the case of an isolated molecule rather than to a molecule in solution.

(16) The fact that the two geminal CH carbons yield a single broad line at −78 °C in toluene but display a pair of equally intense broad lines at the same temperature in $CHF_2Cl/CHFCl_2$ is a consequence of the greater shift separation in this solvent with respect to toluene.

(17) Casarini, D.; Rosini, C.; Grilli, S.; Lunazzi, L.; Mazzanti, A. *J. Org. Chem.* **2003**, *68*, 1815. Lunazzi, L.; Macciantelli, D.; Spunta, G.; Ticca, A. *J. Chem. Soc. Perkin Trans. 2* **1976**, 1791.

**CHART 3**[a]

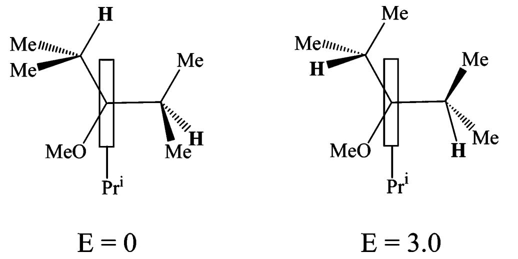


[a] Energies ($E$) are in kcal mol$^{-1}$.

On further cooling the sample below −78 °C, another exchange process is observed: whereas the upfield CH line at 32.7 keeps sharpening as expected, that at lower field (34.2 ppm) broadens further and only at −147 °C becomes as sharp as its upfield companion (at −147 °C the least stable atropisomer has reduced its population to the point of rendering almost invisible the corresponding line, indicated by the diamond). The feature experienced by the 34.2 ppm line is typical of an exchange process between two biased conformers, when one of them is too small to be detected.[18,19] In the present case, this motion is due to the restricted rotation about the C−*i*-Pr bonds of the two diasterotopic geminal isopropyl substituents of the major sc-atropisomer. Calculations predict indeed that there are two possible rotational conformers in the sc-atropisomer of **3**, with one being much more stable than the other, as indicated in Chart 3.

As mentioned above, the rotation about the MeOC−*i*-Pr bond is quite hindered in the ap-atropisomers, but it is much more facile in the less-crowded sc-atropisomer. By making use of the appropriate relationship yielding the rate constant (i.e., $k = \pi\Delta\omega$[20]) at the temperature where the maximum broadening ($\Delta\omega$) is observed for the 34.2 ppm line, an estimate of the $\Delta G^{\ddagger}$ value involving the MeOC−*i*-Pr bond rotation (6.9 ± 0.4 kcal mol$^{-1}$) could be reached also for the sc-atropisomer of **3** (Table 1).

To confirm the interpretation of the processes occurring in **3**, compound **5** was also investigated. The latter bears two geminal isopropyl groups bonded to the MeOC moiety, as in the case of **5**, but it is less-hindered in that it has a methyl, rather than an isopropyl group, in the position 2 of the benzene ring.

Below −40 °C, the $^{13}$C NMR line of the OMe group of **5** splits into two lines, as a result of the two atropisomers in a 74:26 ratio (Figure S1, Supporting Information). They correspond to the sc- and ap-atropisomers: the assignment of the sc-type structure to the major atropisomer was obtained by a NOE experiment carried out at a temperature (−75 °C)[21] where both spectra are distinguishable. Irradiation of the two closely spaced MeO single lines, in fact, enhances the major signal of the methyl in the position 2 of the phenyl ring, whereas the analogous minor signal does not experience any enhancement.

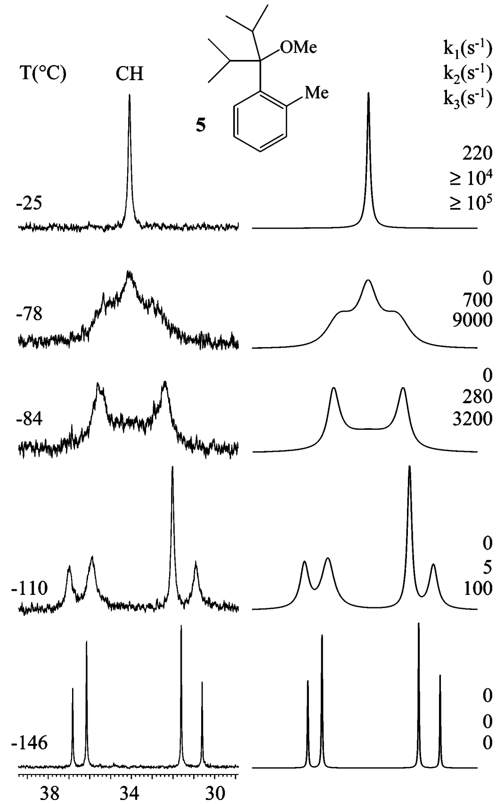


**FIGURE 6.** Left: temperature dependence of the $^{13}$C NMR signals (150.8 MHz in $CHF_2Cl/CHFCl_2$) of the methine carbons of the geminal isopropyl substituents of **5**. Right: line-shape simulations obtained with the rate constants indicated ($k_1$ for the sc to ap interconversion, $k_2$ for the enantiomerization, and $k_3$ for the isopropyl rotation in the minor ap-atropisomer).

A line-shape simulation of the two MeO lines provides a $\Delta G^{\ddagger}$ value of 11.7 kcal mol$^{-1}$ for the sc to ap interconversion barrier (Table 1). When the rate constant ($k_1$) for the sc to ap interconversion becomes negligible on lowering the temperature below −50 °C, additional processes are exhibited by the methine lines of the geminal isopropyl substituents. Both these lines, due to the major sc- and the minor ap-atropisomer, split into 1:1 pairs, thus, eventually displaying four lines at −146 °C, as shown in Figure 6.

In the case of the major sc-atropisomer, this process is due to the slow exchange between the enantiomers +sc and −sc. The line shape simulation ($k_2$ in Figure 6) yields a $\Delta G^{\ddagger}$ value of 8.8 kcal mol$^{-1}$ for the corresponding barrier (Table 1). The splitting of the CH lines observed for the minor ap-atropisomer must have a different origin, because the OMe moiety here is essentially coplanar with the benzene ring. Thus, the diasterotopicity of these CH carbons derives from the restricted rotation of the isopropyl substituents: one isopropyl is in fact locked in a position different from that of the other, as confirmed by the ab initio computation of the ground state of the ap-atropisomer of **5** (Scheme S1, Supporting Information). The barrier for this

(18) (a) Anet, F. A. L.; Yavari, I.; Ferguson, I.; Katritzky, A. R.; Moreno-Mañas, M.; Robinson, M. I. T. *Chem. Commun*. **1976**, 399. Cerioni, G.; Piras, P.; Marongiu, G.; Macciantelli, D.; Lunazzi, L. *J. Chem. Soc., Perkin Trans. 2* **1981**, 1449. Lunazzi, L.; Placucci, G.; Chatgilialoglu, C.; Macciantelli, D. *J. Chem. Soc., Perkin Trans. 2* **1984**, 819. Casarini, D.; Lunazzi, L.; Macciantelli, D. *J. Chem. Soc., Perkin Trans. 2* **1985**, 1839. Lunazzi, L.; Placucci, G.; Macciantelli, D. *Tetrahedron* **1991**, *47*, 6427. Lunazzi, L.; Mazzanti, A.; Casarini, D.; De Lucchi, O.; Fabris, F. *J. Org. Chem* **2000**, *65*, 883. Grilli, S.; Lunazzi, L.; Mazzanti, A. *J. Org. Chem*. **2000**, *65*, 3563.

(19) The fact that the upfield line at 32.7 ppm does not show the same feature as its lowfield companion is because the line of the corresponding invisible conformer has a shift very close to that of the major line.

(20) Anet, F. A. L.; Basus, V. J. *J. Magn. Reson.* **1978**, *32*, 339. Okazawa, N.; Sorensen, T. S. *Can. J. Chem*. **1978**, *56*, 2737. Sandström, J. *Dynamic NMR Sepctroscopy*; Academic Press: New York, 1982; p 94.

(21) A temperature lower than the minimum required to observe separate spectra was employed to avoid saturation transfer effects in the NOE experiment.

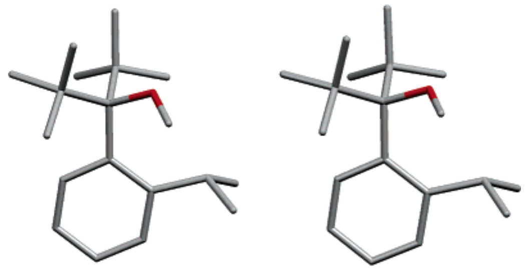


**FIGURE 7.** Experimental X-ray diffraction (left) and ab initio computed (right) structures of **4** (R = *tert*-butyl). The hydrogen atoms are omitted for convenience.

process, as obtained by line-shape simulation ($k_3$ in Figure 6), has been found equal to 7.8 kcal mol$^{-1}$ (Table 1). This value is smaller than that observed in the analogous ap-atropisomer of **3** ($\geq$11.9 kcal mol$^{-1}$) as a result of the greater hindrance exerted in the latter compound by the isopropyl with respect to the methyl group in the position 2 of the phenyl ring.

In the case of compound **4** (R = *tert*-butyl), only one atropisomer was observed; its structure, as assigned by means of a NOE experiment, indicates that the OMe group is directed toward the isopropyl substituent. In fact, irradiation of the OMe signal enhances, in addition to the methyl singlet of the *tert*-butyl group, also the methine and the methyl multiplets of the isopropyl group, whereas no effect is observed for the aromatic signals (Figure S2, Supporting Information). Ab initio computations predict that the C2−C1−C−OMe dihedral angle is 19° in the ground state (see Figure 7), thus indicating that this atropisomer is sp:[22] in addition, the ap-atropisomer is predicted by these calculations to be 5 kcal mol$^{-1}$ less stable than the sp-atropisomer, in agreement with the experimental observation of a single form. The sp structural assignment was further confirmed by single-crystal X-ray diffraction (Figure 7), showing that the C2−C1−C−OMe dihedral angle of **4** is 16° in the solid state.[22]

On lowering the temperature, the $^{13}$C spectrum shows that the quaternary carbon signal of the two *tert*-butyl moieties broadens and splits, at −120 °C, into a pair of 1:1 lines. This is due to the slow interconversion rate between the +sp and −sp enantiomers of **4**: line-shape simulation allowed the measurement of the corresponding barrier ($\Delta G^{\ddagger}$ = 8.4 kcal mol$^{-1}$, as in Table 1). This enantiomerization barrier is lower than that measured in **3** which, in turn, is lower than that measured in **2** (Table 1). This trend confirms that, as previously mentioned, the increasing steric hindrance in **2**, **3**, and **4** destabilizes the ground state more than the transition state.

The low-temperature spectra of the *tert*-butyl methyl groups show that the rotation of the *tert*-butyl group also becomes slow on cooling, thus, six methyl lines are observed at −120 °C. This is because the slow enantiomerization process makes the two *tert*-butyls diastereotopic, and the slow rotation process makes the methyl groups within the two *tert*-butyls diastereotopic. The line-shape simulation (Figure S3, Supporting Information) thus requires that two rate constants be considered. The rate constants for the enantiomerization yield the same barrier as those derived from the two quaternary carbon lines previously mentioned (i.e., 8.4 kcal mol$^{-1}$), and the rate constants for the *tert*-butyl rotation provide a barrier of 9.4 kcal mol$^{-1}$ (Table 1) for this second process.[23]

(22) Because the mentioned dihedral angle is lower than 30°, compound **4** corresponds to an sp-atropisomer, whereas the other compounds investigated here (**1**−**3** and **5**) are labeled sc-atropisomers because their C2−C1−C−OMe dihedral angles are larger than 30°,[11] according to ab initio calculations. The passage from the sc- to the sp-type structure is a consequence of the severe hindrance exerted by the two bulky *tert*-butyl groups present in compound **4**.

## Conclusions

The most populated conformation of the methyl benzyl ethers investigated here (**1**−**5**) is of the sc- or sp-type: only in two cases (**3** and **5**) has the minor form (ap-type) also been detected. Ab initio computations yield a qualitative agreement with the assignments obtained by NOE experiments and X-ray diffraction. The dynamics of the enantiomerization processes occurring in the sc- and sp-atropisomers has been followed by low-temperature NMR and the corresponding barriers determined, with the least-hindered derivative **1** (R = Me) displaying the lowest value (6.6 kcal mol$^{-1}$). Compounds **2**, **3**, and **4** (R = Et, *i*-Pr, and *t*-Bu, respectively), on the other hand, exhibit a trend of the enantiomerization barriers that decreases with the increasing bulkiness of the substituents. This is a consequence of the destabilization of the ground state being larger than that of the transition state as a result of the steric effects of R groups bulkier than methyl.

## Experimental Section

**Materials: 3-(2-Methyl-phenyl)-2,4-dimethyl-pentan-3-ol.** BuLi (1.6 M, 3.1 mL) in hexane was added to a solution of 1-bromo-2-methyl-benzene (5 mmol in 15 mL of dry THF) kept at −78 °C. The solution was stirred for 60 min and treated with 2,4-dimethyl-pentan-3-one (5 mmol in 15 mL of dry THF). After stirring for 10 min, the mixture was warmed to 25 °C, treated with $H_2O$, extracted with $Et_2O$, dried ($Na_2SO_4$), and concentrated at reduced pressure. The crude was purified by a silica gel column (eluent, petroleum ether/$Et_2O$, 9/1) to give the resulting alcohol (1.9 mmol, overall yield 38%); $^1$H NMR ($CDCl_3$, 400 MHz, 25 °C) $\delta$ 0.80 (6H, d, $J$ = 6.5 Hz), 0.91 (6H, d, $J$ = 6.5 Hz), 1.21 (6H, d, $J$ = 6.8 Hz), 1.51 (1H, s, OH), 2.36 (2H, broad), 2.60 (3H, br s, Ar−Me), 7.06−7.24 (4H, m); $^{13}$C NMR ($CDCl_3$, 100.6 MHz, 25 °C) $\delta$ 16.7 (2$CH_3$), 18.0 (2$CH_3$), 24.4 ($CH_3$), 35.5 (CH), 84.2 ($C_q$, broad), 124.6 (CH), 126.1 (CH), 128.0 (CH), 133.0 (CH), 137.6 ($C_q$, broad), 140.4 ($C_q$, broad). Anal. Calcd for $C_{14}H_{21}O$: C, 81.50; H, 10.75. Found: C, 81.58; H, 10.67.

**General Procedure for Compounds 1−5.** A solution of the appropriate alcohol[10] (1 mmol in 2 mL of THF) was slowly added to a suspension of KH kept at −78 °C (5 mmol in 5 mL of anhydrous THF). After 20 min at −78 °C, a solution of MeI (10 mmol in 2 mL of THF) was added, and the mixture was allowed to warm to room temperature and stirred for 10 min. Then the reaction was cautiously quenched with a solution of $NH_4Cl$, extracted with $Et_2O$, and dried on $MgSO_4$. The products were prepurified by chromatography on silica gel (eluent, petroleum ether/$Et_2O$, 19/1); final purification was obtained by semipreparative HPLC (Kromasil-C18 column, 5$\mu$m, 10 × 250 mm, $CH_3CN/H_2O$ 90:10, 5 mL/min). Final yields of the isolated products range from 65 (**1**) to 50% (**4**).

**1-Isopropyl-2-(1-methoxy-1-methyl-ethyl)-benzene (1).** $^1$H NMR ($CDCl_3$, 600 MHz, 25 °C) $\delta$ 1.22 (6H, d, $J$ = 6.9 Hz), 1.62 (6H, s, 2Me), 3.04 (3H, s, OMe), 4.04 (1H, septet, $J$ = 6.9 Hz), 7.15 (1H, dt, $J$ = 7.6 Hz, $J$ = 1.2 Hz), 7.26 (1H, dd, $J$ = 8.0 Hz, $J$ = 1.0 Hz), 7.30 (1H, dt, $J$ = 7.6 Hz, $J$ = 1.0 Hz), 7.41 (1H, dd, $J$ =

(23) Although in principle the rotation barriers might be different for the two diastereotopic *tert*-butyl moieties, such a difference is, in practice, too small to be experimentally detected.

8.0 Hz, $J = 1.2$ Hz); $^{13}$C NMR ($CDCl_3$, 150.8 MHz, 25 °C) $\delta$ 24.3 (Me), 28.2 ($CH_3$), 28.4 (CH), 50.7 ($OCH_3$), 78.6 ($C_q$), 125.3 (CH), 127.4 (CH), 127.7 (CH), 127.9 (CH), 141.0 ($C_q$), 149.6 ($C_q$). Anal. Calcd for $C_{13}H_{20}O$: C, 81.20; H, 10.48. Found: C, 80.88; H, 10.40.

**1-(1-Ethyl-1-methoxy-propyl)-2-isopropyl-benzene (2).** $^1$H NMR ($CDCl_3$, 600 MHz, 25°C) $\delta$ 0.77 (6H, t, $J = 7.5$ Hz), 1.20 (6H, d, $J = 6.8$ Hz), 1.95 (4H, m), 3.01 (3H, s, OMe), 4.08 (1H, septet, $J = 6.8$ Hz), 7.15 (1H, ddd, $J = 7.6$ Hz, $J = 7.5$ Hz, $J = 1.2$ Hz), 7.19 (1H, dd, $J = 8.0$ Hz, $J = 1.0$ Hz), 7.30 (1H, dt, $J = 7.5$ Hz, $J = 1.0$), 7.41 (1H, dd, $J = 8.0$ Hz, $J = 1.2$); $^{13}$C NMR ($CDCl_3$, 150.8 MHz, 25 °C) $\delta$ 7.9 ($CH_3$), 24.8 ($CH_3$), 26.7 ($CH_2$), 28.2 (CH), 50.1 ($OCH_3$), 83.2 ($C_q$), 124.8 (CH), 127.2 (CH), 127.5 (CH), 128.3 (CH), 139.2 ($C_q$), 149.0 ($C_q$). Anal. Calcd for $C_{15}H_{24}O$: C, 81.76; H, 10.98. Found: C, 81.67; H, 10.93.

**1-Isopropyl-2-(1-isopropyl-1-methoxy-2-methyl-propyl)-benzene (3).** $^1$H NMR ($CDCl_3$, 600 MHz, 25 °C) $\delta$ 0.97 (12H, br s), 1.23 (6H, d, $J = 6.9$ Hz), 2.58 (2H, septet, $J = 6.8$ Hz), 3.35 (3H, s, OMe), 3.99 (1H, br s), 7.06 (1H, ddd, $J = 8.4$ Hz, $J = 6.8$ Hz, $J = 1.6$ Hz), 7.15 (1H, br d), 7.30 (1H, dt, $J = 6.8$ Hz, $J = 1.2$ Hz), 7.41 (1H, dd, $J = 7.9$ Hz, $J = 1.6$ Hz); $^{13}$C NMR ($CDCl_3$, 150.8 MHz, 25 °C) $\delta$ 18.6 ($2CH_3$, broad), 19.5 ($2CH_3$), 25.5 ($2CH_3$), 29.1 (CH), 34.0 (2CH, broad), 53.1 ($OCH_3$), 89.0 ($C_q$), 123.9 (CH), 126.4 (CH), 127.7 (CH), 129.6 (CH), 138.1 ($C_q$), 150.2 ($C_q$). Anal. Calcd for $C_{17}H_{29}O$: C, 82.20; H, 11.36. Found: C, 82.33; H, 11.45.

**1-(1-*tert*-Butyl-1-methoxy-2,2-dimethyl-propyl)-2-isopropyl-benzene (4).** $^1$H NMR ($CDCl_3$, 600 MHz, 25 °C) $\delta$ 1.23 (18H, s), 1.29 (6H, d, $J = 6.5$ Hz), 3.43 (3H, s, OMe), 3.89 (1H, septet, $J = 6.8$ Hz), 7.03 (1H, ddd, $J = 8.4$ Hz, $J = 7.1$ Hz, $J = 1.7$ Hz), 7.20 (1H, ddd, $J = 8.0$ Hz, $J = 7.1$ Hz, $J = 1.4$ Hz), 7.39 (1H, dd, $J = 8.0$ Hz, $J = 1.7$ Hz), 7.41 (1H, dd, $J = 8.4$ Hz, $J = 1.4$ Hz); $^{13}$C NMR ($CDCl_3$, 150.8 MHz, 25 °C) $\delta$ 26.7 ($2CH_3$), 28.7 (CH), 31.7 ($6CH_3$), 43.5 ($2C_q$), 57.4 ($OCH_3$), 94.6 ($C_q$), 122.6 (CH), 126.3 (CH), 127.9 (CH), 132.7 (CH), 138.2 ($C_q$), 149.7 ($C_q$). Anal. Calcd for $C_{19}H_{32}O$: C, 82.55; H, 11.67. Found: C, 82.69; H, 11.75.

**1-(1-Isopropyl-1-methoxy-2-methyl-propyl)-2-methyl-benzene (5).** $^1$H NMR ($CDCl_3$, 600 MHz, 25 °C) $\delta$ 0.92 (6H, d, $J = 6.8$ Hz), 0.97 (6H, d, $J = 6.8$ Hz), 2.545 (1H, septet, $J = 6.8$ Hz), 2.555 (3H, s, Ar−Me), 3.35 (3H, s, OMe), 7.08−7.22 (4H, m); $^{13}$C NMR ($CDCl_3$, 150.8 MHz, 25 °C) $\delta$ 17.7 ($2CH_3$), 19.7 ($2CH_3$), 23.5 (Ar−$CH_3$), 34.0 (CH), 53.5 ($OCH_3$), 83.5 ($C_q$, broad), 124.3 (CH), 126.0 (CH), 130.4 (CH), 133.0 (CH), 137.1 ($C_q$, broad), 139.2 ($C_q$, broad). Anal. Calcd for $C_{15}H_{24}O$: C, 81.76; H, 10.98. Found: C, 81.67; H, 10.93.

**NMR Measurements.** NMR spectra were recorded at 600 MHz for $^1$H and 150.8 MHz for $^{13}$C. The assignments of the $^{13}$C signals were obtained by DEPT and two-dimensional experiments (g-HSQC and g-HMBC sequences). The NOE experiments were obtained by means of the double pulse field gradient spin echo-NOE sequence[24] using a "rsnob" selective pulse (typically 37.0 ms, to obtain a 50-Hz-wide pulse), and a mixing time of $^1/_2$ s. The samples for the $^{13}$C NMR low-temperature measurements were prepared by connecting to a vacuum line the NMR tubes containing the compound and some $C_6D_6$ for locking purposes and condensing, therein, the gaseous $CHF_2Cl$ and $CHFCl_2$ under cooling with liquid nitrogen. The tubes were subsequently sealed in vacuo and introduced into the precooled probe of the spectrometer. The temperatures were calibrated by substituting the sample with a precision Cu/Ni thermocouple before the measurements (unless otherwise specified, the errors on the temperature measurements are believed to affect the $\Delta G^\ddagger$ values by ±0.15 kcal mol$^{-1}$). A complete fitting of dynamic NMR line shapes was carried out using a PC version of the DNMR-6 program.[25]

**Computational Details.** Ab initio computations were carried out at the B3LYP/6-31G(d) level by means of the Gaussian 03 series of programs[26] (the standard Berny algoritm in redundant internal coordinates and default criteria of convergence were employed). Harmonic vibrational frequencies were calculated to ascertain the nature of all the stationary points. For each optimized ground state, the frequency analysis showed the absence of imaginary frequencies, whereas for each transition state, the frequency analysis showed a single imaginary frequency. The corresponding optimized structures are reported in the Supporting Information.

**Acknowledgment.** L.L. and A.M. received financial support from the University of Bologna (funds for selected research topics and RFO) and from MIUR-COFIN 2003, Rome (national project "Stereoselection in Organic Synthesis").

**Supporting Information Available:** Figure S1 showing the temperature dependence of the OMe $^{13}$C signal of **5**; Figure S2 showing the NOE spectrum of **4**; Figure S3 showing the temperature dependence of the *tert*-butyl methyl $^{13}$C signals of **4**; Scheme S1 showing the computed structures of the ap- and sc-atropisomers of **5**; X-ray diffraction data of **4**; and ab initio computational data for **1**−**5**. This material is available free of charge via the Internet at http://pubs.acs.org.

JO0603173

(24) (a) Stott, K.; Stonehouse, J.; Keeler, J.; Hwand, T.-L.; Shaka, A. J. *J. Am. Chem. Soc.* **1995**, *117*, 4199. (b) Stott, K.; Keeler, J.; Van, Q. N.; Shaka, A. J. *J. Magn. Reson.* **1997**, *125*, 302. (c) Van, Q. N.; Smith, E. M.; Shaka, A. J. *J. Magn. Reson.* **1999**, *141*, 191. (d) See also: Claridge, T. D. W. *High-Resolution NMR Techniques in Organic Chemistry*; Pergamon: Amsterdam, The Netherlands, 1999.

(25) QCPE program No. 633, Indiana University, Bloomington, IN.

(26) Frisch, M. J.; Trucks, G. W.; Schlegel, H. B.; Scuseria, G. E.; Robb, M. A.; Cheeseman, J. R.; Montgomery, J. A., Jr.; Vreven, T.; Kudin, K. N.; Burant, J. C.; Millam, J. M.; Iyengar, S. S.; Tomasi, J.; Barone, V.; Mennucci, B.; Cossi, M.; Scalmani, G.; Rega, N.; Petersson, G. A.; Nakatsuji, H.; Hada, M.; Ehara, M.; Toyota, K.; Fukuda, R.; Hasegawa, J.; Ishida, M.; Nakajima, T.; Honda, Y.; Kitao, O.; Nakai, H.; Klene, M.; Li, X.; Knox, J. E.; Hratchian, H. P.; Cross, J. B.; Bakken, V.; Adamo, C.; Jaramillo, J.; Gomperts, R.; Stratmann, R. E.; Yazyev, O.; Austin, A. J.; Cammi, R.; Pomelli, C.; Ochterski, J. W.; Ayala, P. Y.; Morokuma, K.; Voth, G. A.; Salvador, P.; Dannenberg, J. J.; Zakrzewski, V. G.; Dapprich, S.; Daniels, A. D.; Strain, M. C.; Farkas, O.; Malick, D. K.; Rabuck, A. D.; Raghavachari, K.; Foresman, J. B.; Ortiz, J. V.; Cui, Q.; Baboul, A. G.; Clifford, S.; Cioslowski, J.; Stefanov, B. B.; Liu, G.; Liashenko, A.; Piskorz, P.; Komaromi, I.; Martin, R. L.; Fox, D. J.; Keith, T.; Al-Laham, M. A.; Peng, C. Y.; Nanayakkara, A.; Challacombe, M.; Gill, P. M. W.; Johnson, B.; Chen, W.; Wong, M. W.; Gonzalez, C.; Pople, J. A. *Gaussian 03*, revision C.02; Gaussian, Inc.: Wallingford, CT, 2004.